Synthesis, Magnetochemistry, and Spectroscopy of Heterometallic Trinuclear Basic Trifluoroacetates $[Fe_2M(\mu_3\text{-}O)(CF_3COO)_6(H_2O)_3]\cdot H_2O$ (M = Mn, Co, Ni)

Konstantin S. Gavrilenko,[a] Attila Vértes,[b] Gyorgy Vanko,[b] Laszlo F. Kiss,[c] Anthony W. Addison,*[d] Thomas Weyhermüller,[e] and Vitaly V. Pavlishchuk*[a]

Keywords: Heterometallic complexes / Carboxylate ligands / Magnetic properties / Iron / Manganese / Cobalt / Nickel / Trinuclear complexes

Three new μ_3-oxo(trifluoroacetato) complexes $[Fe_2^{III}M^{II}(\mu_3\text{-}O)(CF_3COO)_6(H_2O)_3]\cdot H_2O$ [M = Mn (**1**), Co (**2**), Ni (**3**)] have been prepared. Compounds **1** and **2** crystallize in the monoclinic space groups *C*2/*c* [*a* = 22.002(5), *b* = 13.647(3), *c* = 24.767(4) Å, β = 98.23(3)°] and *C*2/*m* [*a* = 21.426(4), *b* = 15.100(2), *c* = 14.815(3) Å, β = 117.99(2)°], respectively. The coordination spheres of the metal ions are essentially octahedral, with the Fe–O distances [1.870(5) Å] falling in the usual range for these systems. Magnetochemical studies reveal the presence of antiferromagnetic exchange in the isosceles triangular skeletons of the polynuclear species. Application of the isotropic spin Hamiltonian $H = -2J_{FeM}[S_{Fe1}S_M + S_MS_{Fe2}] - 2J_{FeFe}[S_{Fe1}S_{Fe2}]$ gives the fitting parameters: $g_{Fe} = g_{Mn} = 2.00$, $J_{Fe\text{-}Fe} = -56.50(7)$ and $J_{Fe\text{-}Mn} = -16.23(4)$ cm^{-1} (**1**), $g_{mol} = 2.09(1)$, $J_{Fe\text{-}Fe} = -42.8(3.5)$ cm^{-1}, $J_{Fe\text{-}Co} = -17.8(1.4)$ cm^{-1} (**2**) and $g_{Fe} = 2.00$, $g_{Ni} = 2.215(2)$, $J_{Fe\text{-}Fe} = -45.60(1)$ and $J_{Fe\text{-}Ni} = -16.96(2)$ cm^{-1} (**3**). A Mössbauer investigation confirms that no electron transfer from Mn^{II} or Co^{II} to Fe^{III} occurs during the syntheses of these complexes.

Introduction

Polynuclear carboxylates of the 3d transition metals have been attracting renewed interest because of their intramolecular magnetic exchange interactions[1,2] and their application as simple models of oligonuclear active sites in metalloproteins.[3−6] Particular attention is being paid to polynuclear complexes behaving as single-molecular magnets.[7−9] Trinuclear (carboxylato)(oxo) complexes are also found within supramolecular arrays of higher nuclearity, and thus are of interest as building blocks ("*molecular Legos*™") with regard to modern magnetic materials.[10,11]

[a] L.V. Pisarzhevskii Institute of Physical Chemistry of the National Academy of Sciences of the Ukraine,
prospekt Nauki 31, 03039 Kiev, Ukraine
Fax: (internat.) + 38-044/265-6216
E-mail: pavlisvv@phyche.freenet.kiev.ua
[b] Research Group for Nuclear Techniques in Structural Chemistry of the Hungarian Academy of Sciences at Eötvös University of Budapest
Pf. 32, 1518 Budapest 112, Hungary
Fax: (internat.) + 36-1/209-0602
E-mail: vertesa@ludens.elte.hu
[c] Research Institute for Solid State Physics and Optics
P. O. Box 49, 1121 Budapest, Hungary
Fax: (internat.) + 36-1/395-9278
E-mail: kiss@power.szfki.kfki.hu
[d] Department of Chemistry, Drexel University,
Philadelphia, PA 19104, U.S.A.
Fax: (internat.) + 1-215/895-1265
E-mail: addisona@drexel.edu
[e] Max-Planck Institut für Strahlenchemie,
Stiftstraße 34−36, 45470 Mülheim, Germany
Fax: (internat.) + 49-208/306-3951
E-mail: weyherm@mpi-muelheim.mpg.de

The first heterometallic trinuclear acetates of tripositive iron and chromium $[X_2^{III}Z^{III}(\mu_3\text{-}O)(CH_3COO)_6(H_2O)_3]^+$ (where X_2Z = Fe_2Cr, Cr_2Fe)[12] and of mixed-valence metals $[Fe_2^{III}M^{II}(\mu_3\text{-}O)(CH_3COO)_6(H_2O)_3]$ (where M = Co, Mn, Ni, Zn)[13] were synthesized by Weiland. Difficulties in the synthesis and in the interpretation of the physicochemical properties of these heterometallic trinuclear carboxylates discouraged their extensive investigation.[14] Nonetheless, the consequences of straightforward variations in their structures, such as substitution of the acetate group by other functionalised carboxylates, appear to be fundamental in the development of new materials derived from them. This class of compounds is also active with respect to alkane activation, the catalytic activity being dependent on the carboxylate and metal identities.[15,16]

Thus, it is attractive to combine this property of superacidity and catalytic activity of trinuclear (carboxylato)(μ_3-oxo) complexes using strong acids such as trifluoroacetic acid as the ligand source. We present here the syntheses, structures and investigation of the spectroscopic and magnetic behaviour of the trinuclear heterometallic basic trifluoroacetates $[Fe_2^{III}M^{II}(\mu_3\text{-}O)(CF_3COO)_6(H_2O)_3]$ (M = Mn, Co, Ni).

Results and Discussion

Synthesis

The heteronuclear basic trifluoroacetates $[Fe_2^{III}M^{II}(\mu_3\text{-}O)(CF_3COO)_6(H_2O)_3]\cdot H_2O$ [M = Mn (**1**), Co (**2**), Ni (**3**)]

were synthesized by metathesis reaction between trifluoroacetate and the acetate trimers. The reactions proceeded smoothly in aqueous trifluoroacetic acid as the solvent without any destruction of the oxo-bridged trinuclear skeleton of the Mn, Co, or Ni complexes, despite the substantial acidity of trifluoroacetic acid [Equation (1)].

$$[Fe_2^{III}M^{II}(\mu_3\text{-}O)(CH_3COO)_6(H_2O)_3]\cdot 3H_2O + 6\,CF_3COOH \rightarrow [Fe_2^{III}M^{II}(\mu_3\text{-}O)(CF_3COO)_6(H_2O)_3]\cdot H_2O + 6\,CH_3COOH + 2\,H_2O \quad (1)$$

Similar metathesis reactions have also been applied successfully to higher-nuclearity carboxylates.[17] All the trifluoroacetate compounds are readily soluble in water and a variety of organic solvents, so that growing single crystals of **1**−**3** by concentration, vapour diffusion or liquid diffusion was limited to certain solvent combinations, as reflected by the compositions of the crystals described below.

Description of Structures

Molecular structures of $[Fe_2Mn(\mu_3\text{-}O)(CF_3COO)_6(H_2O)_3]\cdot 2MeNO_2\cdot H_2O$ (**1′**) and $[Fe_2Co(\mu_3\text{-}O)(CF_3COO)_6(H_2O)_3]\cdot 3Me_2CO\cdot 1/2Mes$ (**2′**) were examined under cryogenic conditions (100 K). An ORTEP diagram of $[Fe_2Co(\mu_3\text{-}O)(CF_3COO)_6(H_2O)_3]$ is presented in Figure 1. The principal lattice matrices of the complexes are listed in Table 6, while bond lengths and angles of **2′** are presented in Table 1.

$[Fe_2Co(\mu_3\text{-}O)(CF_3COO)_6(H_2O)_3]\cdot 3Me_2CO\cdot 1/2Mes$ (Mes = 1,3,5-trimethylbenzene) (2′)

The monoclinic unit cell of the complex contains 4 molecules of the trinuclear complex, 12 molecules of acetone, and 2 molecules of mesitylene. In the crystal structure of **2′**, all the trinuclear molecules are located in parallel layers of sequence *ABAB*. Hence the molecules of the third layer occupy positions precisely above those of the first layer. The absence of interlayer trimer−trimer cohesion forces (e.g. through the lack of any intertrimer hydrogen bonds) allows the solvent molecules to readily penetrate and occupy the interlayer volume. The interstices between trinuclear species are occupied by molecules of acetone and mesitylene, the aromatic ring planes of mesitylene being perpendicular to the trimetal planes. The *R* factor (0.0857) for this structure is somewhat raised by the disorder in the trifluoromethyl groups, as well as in the mesitylene (lying on the C_2 axes) and acetone molecules (lying on the symmetry planes).

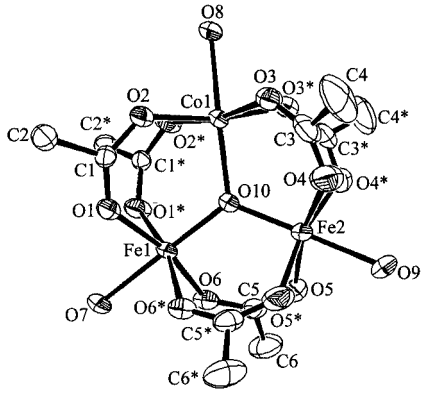

Figure 1. ORTEP plot of the structure of the skeleton of complex **1′**; thermal ellipsoids are shown at the 20% level for clarity; H and F atoms are omitted for clarity of presentation

Table 1. Selected distances and angles in $[Fe_2Co(\mu_3\text{-}O)(CF_3COO)_6(H_2O)_3]\cdot 3Me_2CO\cdot 1/2Mes$

Distances [Å]			
Fe1−Fe2	3.26(1)	Fe2−O4	2.030(4)
Fe1−Co	3.33(1)	Fe2−O4*[a]	2.030(4)
Fe2−Co	3.33(1)	Fe2−O5	2.049(4)
Fe1−O10	1.873(5)	Fe2−O5*	2.049(4)
Fe1−O1	2.028(6)	Fe2−O9	2.079(5)
Fe1−O1*	2.028(6)	Co−O10	1.993(5)
Fe1−O6	2.076(6)	Co−O2	2.069(4)
Fe1−O6*	2.076(6)	Co−O2*	2.069(4)
Fe1−O7	2.080(7)	Co−O3*	2.078(4)
Fe2−O10	1.867(5)	Co−O3	2.078(4)
		Co−O8	2.076(6)
Angles [°]			
Fe1−O10−Fe2	121.5(3)	O4*−Fe2−O5*	88.6(2)
Fe1−O10−Co	119.1(3)	O4−Fe2−O5*	166.7(2)
Fe2−O10−Co	119.4(3)	O4−Fe2−O9	83.6(2)
O10−Fe1−O1	96.6(2)	O4*−Fe2−O5	166.7(2)
O10−Fe1−O1*	96.6(2)	O4−Fe2−O5	88.6(2)
O10−Fe1−O6	95.8(2)	O4*−Fe2−O9	83.6(2)
O10−Fe1−O6*	95.8(2)	O5*−Fe2−O5	90.6(2)
O10−Fe1−O7	178.8(3)	O5−Fe2−O9	83.2(2)
O1−Fe1−O1*	91.1(4)	O5*−Fe2−O9	83.2(2)
O1*−Fe1−O6*	89.3(2)	O10−Co1−O2	94.3(2)
O1−Fe1−O6*	167.5(2)	O10−Co1−O2*	94.3(2)
O1*−Fe1−O7	84.3(2)	O10−Co1−O8	178.1(2)
O1*−Fe1−O6	167.5(2)	O10−Co1−O3	95.4(2)
O1−Fe1−O6	89.3(2)	O10−Co1−O3*	95.4(2)
O1−Fe1−O7	84.3(2)	O2−Co1−O2*	90.0(2)
O6*−Fe1−O6	87.6(3)	O2*−Co1−O8	84.4(2)
O6−Fe1−O7	83.3(2)	O2*−Co1−O3*	91.7(2)
O6*−Fe1−O7	83.3(2)	O2−Co1−O3*	170.0(2)
O10−Fe2−O4	97.2(2)	O2−Co1−O8	84.4(2)
O10−Fe2−O4*	97.2(2)	O2*−Co1−O3	170.0(2)
O10−Fe2−O5	96.1(2)	O2−Co1−O3	91.7(2)
O10−Fe2−O5*	96.1(2)	O8−Co1−O3	85.9(2)
O10−Fe2−O9	178.9(2)	O8−Co1−O3*	85.9(2)
O4−Fe2−O4*	89.1(3)	O3*−Co1−O3	84.9(3)

[a] The positions of the atoms with an asterisk are defined by the appropriate symmetry operations. The standard deviations are reported in parentheses.

The molecular structure of the complex is based on an isosceles triangular Fe_2Co fragment, with a μ_3-bridging oxide oxygen atom μ_3-O(O10) at the centre of the triangle made up by two iron(III) atoms and a cobalt(II) atom. Six μ-trifluoroacetate anions also join the metal atoms through carboxylate oxygen atoms (O_c), reinforcing the triangular framework: in each case the carboxylate groups have a μ-O,O′ coordination. The oxygen donor atoms of the water molecules bring the coordination number of each metal 3d-ion to 6, so that each Fe^{3+} and Co^{2+} ion manifests a distorted octahedral environment of oxygen atoms. The coplanarity of the μ_3-oxygen atom with the triangle of the

metal ions shows that it is an sp^2-hybridised oxide ion, removing the ambiguity associated with a possible μ_3-OH^- bridge. The average μ_3-O−Fe distance of 1.870(5) Å is typical for $Fe^{3+}-O^{2-}$ bonds in trinuclear (carboxylato)(μ_3-oxo) complexes.[18] Comparison of this value with corresponding distances in $[Fe^{III}_2Fe^{II}(\mu_3\text{-}O)(CH_3COO)_6(4\text{-Et-py})_3]$ (μ_3-O−Fe^{2+} 2.01 Å, μ_3-O−Fe^{3+}, 1.86 Å at 163 K)[19] favours the assumption that the oxidation state of the iron atoms in **2** remains +3. If the μ_3-O^{2-} ionic radius is taken as 1.22 Å,[20] the ionic radius of Fe^{3+} can be estimated to be 0.64 Å, somewhat smaller than the value reported at room temperature (0.78 Å[20]). The μ_3-O−Co distance [1.993(5) Å] is greater than μ_3-O−Fe, due to the larger ionic radius of Co^{2+}.[20] For each Fe^{3+} ion, three sets of values of the Fe−O bond lengths are found: short μ_3-O−Fe distances (1.87 Å), two intermediate Fe−O_c distances (2.03 Å for Fe−O1 and Fe1−O1*), and three longer Fe−O_c and Fe−OH_2 bonds (ranging from 2.05 Å for Fe2−O5 and Fe2−O5*, to 2.08 Å for Fe1−O7 and Fe2−O9, where O_c are oxygen atoms of the carboxylate bridges). For the Co^{2+} ion, the differences between the Co−O_c bond lengths [2.069(4) and 2.078(4) Å] are less significant than the corresponding bond lengths in analogous trinuclear acetato complexes. This can be rationalised by a weaker donor power of the trifluoroacetate ion (due to the inductive effect of the CF_3− group) in comparison with the acetate group. All the M−OH_2 bond lengths are 2.08 Å.

In the acetato complex $[Fe_2Co(\mu_3\text{-}O)(CH_3COO)_6(H_2O)_3]\cdot 2H_2O$, which crystallises in a monoclinic system ($Z = 8$),[21] disorder causes the metal atoms to appear to be arranged at the corners of an equilateral triangle, hence concealing the identities of the individual Fe^{3+} and Co^{2+} ions. In the present trifluoroacetate case, the observed C_{2v} symmetry of the trimetal unit allows the distinction between Fe^{3+} and Co^{2+} to be made.

$[Fe_2Mn(\mu_3\text{-}O)(CF_3COO)_6(H_2O)_3]\cdot 2MeNO_2\cdot H_2O$ (**1′**)

This complex also crystallises in a monoclinic space group. The parallel layers of trinuclear species are arranged in an *ABCDEABCDE* sequence. The overall *R* factor for the structure is quite large because of substantial disordering of the trifluoromethyl groups and solvent molecules. However, the trinuclear skeleton is confirmed and certain details are clearly apparent. The structure of **1′** is not identical to that of **2′**, the trimetal moiety forms a slightly distorted isosceles triangle: [Fe1−Mn 3.328(2) Å; Fe2−Mn 3.368(2) Å; Fe−Fe 3.273(2) Å]. The coordination spheres of the metal ions are essentially octahedral, with the Fe−μ_3-O distances in the typical range for these systems: the μ_3-O−Fe bond lengths (1.86 and 1.87 Å for atoms Fe1 and Fe2, respectively) differ slightly from the corresponding values in **2′**, while a similar effect is seen for the Fe−OH_2 bond (2.10 and 2.06 Å for Fe1 and Fe2, respectively). The Fe−O_c distances vary from 2.01 to 2.07 Å, similar Fe−O_c distances have been found in analogous compounds.[22] Meanwhile, the μ_3-O−Mn (2.02 Å), Mn−O_c and Mn−OH_2 distances (2.11−2.15 Å) are in a range consistent with the persistence of Mn^{2+} under the conditions of synthesis. In consonance with this, the Mössbauer spectrum of this compound (vide infra) testifies to the presence of iron(III) rather than iron(II) in **1′**.

Mass Spectra

FAB mass spectra clearly indicate the trinuclear nature of complexes **1**−**3**, as well as the persistence of the $Fe_2M^{II}(\mu_3\text{-}O)$ skeletons. Although ions such as $[Fe_2M^{II}(\mu_3\text{-}O)(CF_3COO)_6(H_2O)_2]^+$ or $[Fe_2M^{II}(\mu_3\text{-}O)(CF_3COO)_5]^+$ are not immediately apparent, intense peaks associated with partially solvated $[Fe_2M^{II}(\mu_3\text{-}O)(CF_3COO)_5(H_2O)_2]^+$ cations are present in each case (Table 2). The spectra also display fragmentation patterns corresponding to consecutive loss of trifluoroacetate groups and water molecules. The relative intensities suggest a greater lability for trifluoroacetate than for water.

Table 2. FAB-MS data for the complexes $[Fe_2M(\mu_3\text{-}O)(CF_3COO)_6(H_2O)_3]\cdot H_2O$ (M = Mn, Co, Ni)

Ion composition	*m/z*		
	Mn	Co	Ni
$[Fe_2M(\mu_3\text{-}O)(CF_3COO)_5(H_2O)_2]^+$	787	791	790
$[Fe_2M(\mu_3\text{-}O)(CF_3COO)_5]^+$	748	752	–
$[Fe_2M(\mu_3\text{-}O)(CF_3COO)_4(H_2O)_2]^+$	674	678	677
$[Fe_2M(\mu_3\text{-}O)(CF_3COO)_4]^+$	635	639	638
$[Fe_2M(\mu_3\text{-}O)(CF_3COO)_3(H_2O)]^+$	541	545	544
$[Fe_2M(\mu_3\text{-}O)(CF_3COO)_3]^+$	522	526	525
$[Fe_2M(\mu_3\text{-}O)(CF_3COO)_2(H_2O)_2]^+$	447	451	450
$[Fe_2M(\mu_3\text{-}O)(CF_3COO)_2(H_2O)]^+$	428	432	431
$[Fe_2M(\mu_3\text{-}O)(CF_3COO)(H_2O)_2]^+$	334	338	337

IR Spectra

The IR absorption bands for **1**−**3** (Table 3) are consistent with those reported in the literature for the acetate analogues[22,23] and are similarly assigned: $\nu(COO^-)_s$ and $\nu(COO^-)_{as}$ in **1**−**3** are shifted to a lower energy by 40−50 cm^{-1} relative to the trinuclear basic acetates,[22] indicating

Table 3. IR data for trinuclear carboxylates [cm^{-1}]

Complex	$\nu(M_3O)_{as}$	$\nu(COO^-)_s$	$\nu(COO^-)_{as}$	$\Delta\nu$[a]
$[Fe_2Mn(\mu_3\text{-}O)(CF_3COO)_6(H_2O)_3]\cdot H_2O$	622	1470	1640	170
$[Fe_2Co(\mu_3\text{-}O)(CF_3COO)_6(H_2O)_3]\cdot H_2O$	627	1475	1630	155
$[Fe_2Ni(\mu_3\text{-}O)(CF_3COO)_6(H_2O)_3]\cdot H_2O$	630	1475	1645	170

[a] $\Delta\nu = \nu(COO^-)as - \nu(COO^-)s$.

that the replacement of the CH_3 radical by the more powerfully electron-accepting CF_3 moiety weakens the metal$-O_c$ force constant.

The splitting of the symmetric and asymmetric valence vibrations ($\Delta\nu$, Table 3) signals bidentate bridging carboxylate groups around the $Fe_2M(\mu_3\text{-}O)$ fragment,[12] while the bands at 600−650 cm^{-1} are assigned to vibrations of the $Fe_2M(\mu_3\text{-}O)$ skeleton.

Electronic Spectra

The electronic spectra of **1**−**3** (Table 4) are similar to those reported for other trinuclear basic carboxylates containing iron(III),[22] and are useful in revealing the spin states of the metal ions. At longer wavelengths, absorbance bands are observed which are characteristic of d−d transitions from the $^6A_{1g}$ ground state of a distorted octahedral high-spin Fe^{3+} ion. For instance, the band at 17500 cm^{-1} is assigned to the $^6A_{1g}\rightarrow{}^4A_{2g}$ d−d transition, the intensity of which is enhanced due to the influence of exchange interactions[24] inside the trinuclear moiety. The remaining Fe^{3+} d−d transitions are obscured by intense absorbance bands near 29000 and 22000 cm^{-1} (ε = 1500−3000 $dm^3\cdot mol^{-3}\cdot cm^{-1}$) associated with the ligand-to-metal charge-transfer transitions which are characteristic of such iron(III) systems.[25,26] The electronic spectrum of $[Fe_2Ni(\mu_3\text{-}O)(CF_3COO)_6(H_2O)_3]\cdot H_2O$ (**3**) exhibits an absorbance band at 13580 cm^{-1} (Table 4). The position and intensity of this band are consistent with a $^3A_{2g}\rightarrow{}^3T_{2g}$ assignment for an octahedral Ni^{2+} chromophore.[25] The intensity of this band in **3** is slightly enhanced relative to similar bands in mononuclear Ni^{2+} complexes, which is likely to be related to the exchange interactions in the $Fe_2Ni^{2+}(\mu_3\text{-}O)$ moiety.[24] Literature data for various other basic carboxylates[22,24] also confirm that the exchange interactions are generally orders of magnitude less than the differences amongst the term energies of the individual ions.

Table 4. UV/VIS spectra of the trinuclear complexes in acetonitrile solution

Complex	λ_{max} [cm^{-1}] (ε[a] [L cm^{-1} mol^{-1}])
$[Fe_2Mn(\mu_3\text{-}O)(CF_3COO)_6(H_2O)_3]\cdot H_2O$	29200 (3970), 25640 (540) sh, 21490 (223), 17420 (103) sh
$[Fe_2Co(\mu_3\text{-}O)(CF_3COO)_6(H_2O)_3]\cdot H_2O$	29600 (3655), 22330 (1356), 17400 (368)
$[Fe_2Ni(\mu_3\text{-}O)(CF_3COO)_6(H_2O)_3]\cdot H_2O$	28640 (2450), 17600 (309), 13580 (36)

[a] Molar extinction coefficient in parentheses.

Magnetic Studies

Temperature dependencies of the magnetic susceptibilities of complexes **1**−**3** were measured in the 5−300 K range.

Complex $[Fe_2Mn(\mu_3\text{-}O)(CF_3COO)_6(H_2O)_3]\cdot H_2O$ (1)

With decreasing temperature, $\chi_M T$ (in $cm^3\cdot K\cdot mol^{-1}$, where χ_M is per mol of trimer) decreased smoothly from 4.51 at 300 K to 3.19 at 5 K (Figure 2). The observed $\chi_M T$ value for this complex, even at room temperature, is significantly lower than the expected spin-only $\chi_M T$ value (13.125 $cm^3\cdot K\cdot mol^{-1}$) for a non-interacting $g = 2$ high-spin set of one manganese(II) and two iron(III) ions. This clearly indicates strong antiferromagnetic coupling within the Fe_2Mn framework. In general, two high-spin iron(III) ions with $S = 5/2$ and one manganese(II) ion with $S = 5/2$ can couple to give a total molecular spin (S_T) ranging from 1/2 to 15/2. Magnetic data were analysed according to the exchange Hamiltonian [Equation (2)], and the coupling pathways are presented in Scheme 1.

$$H = -2J_{FeM}[S_{Fe1}S_M + S_MS_{Fe2}] - 2J_{FeFe}[S_{Fe1}S_{Fe2}] \quad (2)$$

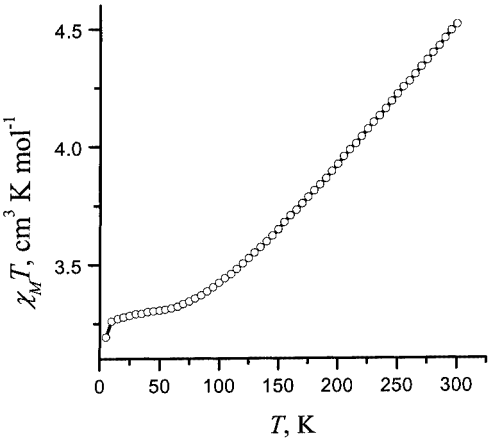

Figure 2. Temperature dependence of the magnetic susceptibility of **1**, plotted as χT vs. T; the solid line is the least-squares fit

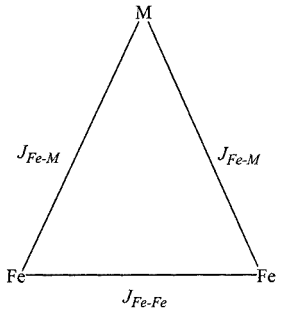

Scheme 1. Magnetic exchange pathways in the trinuclear core

The zero-field energy levels for the Fe_2M complexes were calculated according to Equation (3),[5] where $S_{Fe} = 5/2$; S_M is the spin of M^{II} (5/2 for Mn^{II}, 3/2 for Co^{II}, and 2/2 for Ni^{II}); $S^* = S_{Fe} + S_{Fe}$; $S_T = S^* + S_M$ according to Kambe's notation.[27]

$$E(S_T, S^*) = J_{FeM}[2S_{Fe}(S_{Fe} + 1) - S_T(S_T + 1)] + J_{FeFe}[S_T(S_T + 1) + S_M(S_M + 1) - S^*(S^* + 1)] \quad (3)$$

Within this approach, S^* ranges integrally from 0 to 5, so that for instance, when $S^* = 1$, S_T for the Co^{II}-containing molecule may take values of 1/2, 3/2, or 5/2. Substitution

of the eigenvalues for the spin-states derived from the above exchange Hamiltonian into the van Vleck equation results in an expression for the $\chi_M T$ values for the Fe_2Mn complex [Equation (4)], where $a = -25J_{Fe\text{-}Mn} - 12.5J_{Fe\text{-}Fe}$; $b = -10J_{Fe\text{-}Mn} - 12.5J_{Fe\text{-}Fe}$; $c = 3J_{Fe\text{-}Mn} - 12.5J_{Fe\text{-}Fe}$; $d = 14J_{Fe\text{-}Mn} - 12.5J_{Fe\text{-}Fe}$; $e = 23J_{Fe\text{-}Mn} - 12.5J_{Fe\text{-}Fe}$; $f = 30J_{Fe\text{-}Mn} - 12.5J_{Fe\text{-}Fe}$; $\gamma = -20J_{Fe\text{-}Mn} - 2.5J_{Fe\text{-}Fe}$; $h = -7J_{Fe\text{-}Mn} - 2.5J_{Fe\text{-}Fe}$; $\omega = 4J_{Fe\text{-}Mn} - 2.5J_{Fe\text{-}Fe}$; $j = 13J_{Fe\text{-}Mn} - 2.5J_{Fe\text{-}Fe}$; $\kappa = 20J_{Fe\text{-}Mn} - 2.5J_{Fe\text{-}Fe}$; $l = 25J_{Fe\text{-}Mn} - 2.5J_{Fe\text{-}Fe}$; $m = -15J_{Fe\text{-}Mn} + 5.5J_{Fe\text{-}Fe}$; $n = -4J_{Fe\text{-}Mn} + 5.5J_{Fe\text{-}Fe}$; $o = 5J_{Fe\text{-}Mn} + 5.5J_{Fe\text{-}Fe}$; $p = 12J_{Fe\text{-}Mn} + 5.5J_{Fe\text{-}Fe}$; $q = 17J_{Fe\text{-}Mn} + 5.5J_{Fe\text{-}Fe}$; $r = 20J_{Fe\text{-}Mn} + 5.5J_{Fe\text{-}Fe}$; $s = -10J_{Fe\text{-}Mn} + 11.5\ J_{Fe\text{-}Fe}$; $t = -J_{Fe\text{-}Mn} + 11.5J_{Fe\text{-}Fe}$; $u = 6J_{Fe\text{-}Mn} + 11.5J_{Fe\text{-}Fe}$; $v = 11J_{Fe\text{-}Mn} + 11.5J_{Fe\text{-}Fe}$; $w = 14J_{Fe\text{-}Mn} + 11.5J_{Fe\text{-}Fe}$; $x = -5J_{Fe\text{-}Mn} + 15.5J_{Fe\text{-}Fe}$; $y = 2J_{Fe\text{-}Mn} + 15.5J_{Fe\text{-}Fe}$; $z = -7J_{Fe\text{-}Mn} + 15.5J_{Fe\text{-}Fe}$; $\varphi = 17.5J_{Fe\text{-}Fe}$.

$$\chi_M T = (Ng^2\beta^2/3k)(1020e^{-a/kT} + 682.5e^{-b/kT} + 429e^{-c/kT} + 247.5e^{-d/kT} + 126e^{-e/kT} + 52.5e^{-f/kT} + 682.5e^{-\gamma/kT} + 429e^{-h/kT} + 247.5e^{-\omega/kT} + 126e^{-j/kT} + 52.5e^{-\kappa/kT} + 15e^{-l/kT} + 429e^{-m/kT} + 247.5e^{-n/kT} + 126e^{-o/kT} + 52.5e^{-p/kT} + 15e^{-q/kT} + 1.5e^{-r/kT} + 247.5e^{-s/kT} + 126e^{-t/kT} + 52.5e^{-u/kT} + 15e^{-v/kT} + 1.5e^{-w/kT} + 126e^{-x/kT} + 52.5e^{-y/kT} + 15e^{-z/kT} + 52.5e^{-\varphi/kT})/(16e^{-a/kT} + 14e^{-b/kT} + 12e^{-c/kT} + 10e^{-d/kT} + 8e^{-e/kT} + 6e^{-f/kT} + 14e^{-\gamma/kT} + 12e^{-h/kT} + 10e^{-\omega/kT} + 8e^{-j/kT} + 6e^{-\kappa/kT} + 4e^{-l/kT} + 12e^{-m/kT} + 10e^{-n/kT} + 8e^{-o/kT} + 6e^{-p/kT} + 4e^{-q/kT} + 2e^{-r/kT} + 10e^{-s/kT} + 8e^{-t/kT} + 6e^{-u/kT} + 4e^{-v/kT} + 2e^{-w/kT} + 8e^{-x/kT} + 6e^{-y/kT} + 4e^{-z/kT} + 6e^{-\varphi/kT}) \quad (4)$$

Despite the deviation of this complex from an exact isosceles triangle, a satisfactory fit was achieved using two J parameters. The best fit was obtained with fixed values of $g_{Fe} = g_{Mn} = 2.00$, giving $J_{Fe\text{-}Fe} = -56.50(7)$ and $J_{Fe\text{-}Mn} = -16.23(4)$ cm^{-1} [$R^2 = 1.85\cdot10^{-5}$ where $R^2 = \Sigma(\chi_{obs}-\chi_{calc})^2/\Sigma\chi^2_{obs}$]. An energy diagram (Figure 3) for the spin states of **1** reveals that the ground state is a quadruplet (S_T, S^*) = (3/2, 1), with a low-lying sextuplet (5/2, 0) 0.61 cm^{-1} above it. The experimental $\chi_M T$ value at 5 K (3.19) is intermediate between the calculated values for these two spin-states: 1.88 cm^3·K·mol^{-1} for a quadruplet and 4.38 cm^3·K·mol^{-1} for a sextuplet ground state, and the $\chi_M T$ data thus betoken Boltzmann distribution over these two states. Previously, Blake et al. reported that $S_T = 3/2$ is the ground state for $[Fe_2Mn(\mu_3\text{-}O)(CH_3COO)_6(py)_3]\cdot0.7py$.[24]

Complex $[Fe_2Co(\mu_3\text{-}O)(CF_3COO)_6(H_2O)_3]\cdot H_2O$ (2)

In general, the magnetic properties of **2** resembled those of the manganese analogue (Figure 4). On cooling, $\chi_M T$ for this complex decreased from 4.76 cm^3·K·mol^{-1} at 300 K to 2.00 at 5 K (Figure 4). The observed χ_MT value at room temperature is less than one half of the spin-only χ_MT value (10.61 cm^3·K·mol^{-1}) for a non-interacting FeCoFe ion set. Again, this directly testifies for the existence of strong antiferromagnetic coupling within the Fe_2Co framework. Two high-spin irons(III) ions and one high-spin ($S = 3/2$) cobalt(II) ion can couple to give spins ranging from $S_T = 1/2$ to $S_T = 13/2$. The experimental data were fitted according to the isotropic spin-Hamiltonian [Equation (2)] to give Equation (5), where $a = -15J_{Fe\text{-}Co} - 12.5J_{Fe\text{-}Fe}$; $b = -2J_{Fe\text{-}Co} - 12.5J_{Fe\text{-}Fe}$; $c = 9J_{Fe\text{-}Co} - 12.5J_{Fe\text{-}Fe}$; $d = 18J_{Fe\text{-}Co} - 12.5J_{Fe\text{-}Fe}$; $e = -12J_{Fe\text{-}Co} - 2.5J_{Fe\text{-}Fe}$; $f = -J_{Fe\text{-}Co} - 2.5J_{Fe\text{-}Fe}$; $\gamma = 8J_{Fe\text{-}Co} - 2.5J_{Fe\text{-}Fe}$; $h = 15J_{Fe\text{-}Co} - 2.5J_{Fe\text{-}Fe}$; $\omega = -9J_{Fe\text{-}Co} + 5.5J_{Fe\text{-}Fe}$; $j = 5.5J_{Fe\text{-}Fe}$; $\kappa = 7J_{Fe\text{-}Co} + 5.5J_{Fe\text{-}Fe}$; $l = 12J_{Fe\text{-}Co} + 5.5\ J_{Fe\text{-}Fe}$; $m = -6\ J_{Fe\text{-}Co} + 11.5J_{Fe\text{-}Fe}$; $n = J_{Fe\text{-}Co} + 11.5J_{Fe\text{-}Fe}$; $o = 6J_{Fe\text{-}Co} + 11.5J_{Fe\text{-}Fe}$; $p = 9J_{Fe\text{-}Co} + 11.5J_{Fe\text{-}Fe}$; $q = -3J_{Fe\text{-}Co} + 15.5J_{Fe\text{-}Fe}$; $r = 2J_{Fe\text{-}Co} + 15.5J_{Fe\text{-}Fe}$; $s = 5J_{Fe\text{-}Co} + 15.5J_{Fe\text{-}Fe}$; $t = 17.5J_{Fe\text{-}Fe}$.

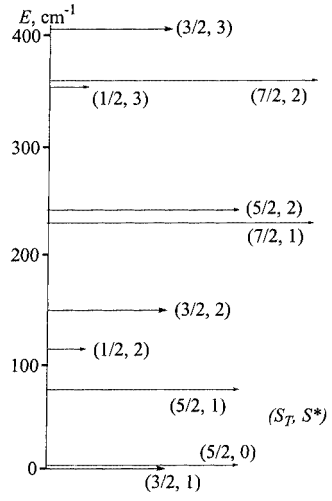

Figure 3. Energy diagram for low-lying spin levels of **1**

$$S_T = [(Ng_{mol}^2\beta^2/3k)(682.5e^{-a/kT} + 429e^{-b/kT} + 247.5e^{-c/kT} + 126e^{-d/kT} + 429e^{-e/kT} + 247.5e^{-f/kT} + 126e^{-\gamma/kT} + 52.5e^{-h/kT} + 247.5e^{-\omega/kT} + 126e^{-j/kT} + 52.5e^{-\kappa/kT} + 15e^{-l/kT} + 126e^{-m/kT} + 52.5e^{-n/kT} + 15e^{-o/kT} + 1.5e^{-p/kT} + 52.5e^{-q/kT} + 15e^{-r/kT} + 1.5e^{-s/kT} + 15e^{-t/kT})/(14e^{-a/kT} + 12e^{-b/kT} + 10e^{-c/kT} + 8e^{-d/kT} + 12e^{-e/kT} + 10e^{-f/kT} + 8e^{-g/kT} + 6e^{-h/kT} + 10e^{-\omega/kT} + 8e^{-j/kT} + 6e^{-\kappa'/kT} + 4e^{-l/kT} + 8e^{-m/kT} + 6e^{-n/kT} + 4e^{-o/kT} + 2e^{-p/kT} + 6e^{-q/kT} + 4e^{-r/kT} + 2e^{-s/kT} + 4e^{-t/kT})](1 - \rho) + S(S+1)(Ng^2\beta^2/3k)\rho + TIP \quad (5)$$

Here, ρ is the fraction of a mononuclear ferric paramagnetic ($S = 5/2$) impurity, and g_{mol} is for the trinuclear complex.

The best fit was obtained with $g_{mol} = 2.09(1)$; $J_{Fe\text{-}Fe} = -42.8(3.5)$ cm^{-1}; $J_{Fe\text{-}Co} = -17.8(1.4)$ cm^{-1}; $\rho = 0.031(5)$ and $TIP = 0$ ($R^2 = 6.17\cdot10^{-6}$). Fixing g_{Fe} at 2.00 gave $g_{Co} = 2.27$ according to $3g_{mol} = (2\ g_{Fe} + g_{Co})$. The associated spin ladder energy diagram reveals a (1/2, 1) ground state with a (3/2, 0) state 3.2 cm^{-1} above it (Figure 5). These states are well-separated from the second excited state (3/2, 1), which is 50 cm^{-1} above them.

Complex $[Fe_2Ni(\mu_3\text{-}O)(CF_3COO)_6(H_2O)_3]\cdot H_2O$ (3)

For this complex, the $\chi_M T$ value monotonically decreased from 3.03 cm^3·K·mol^{-1} at 300 K to about 1.15

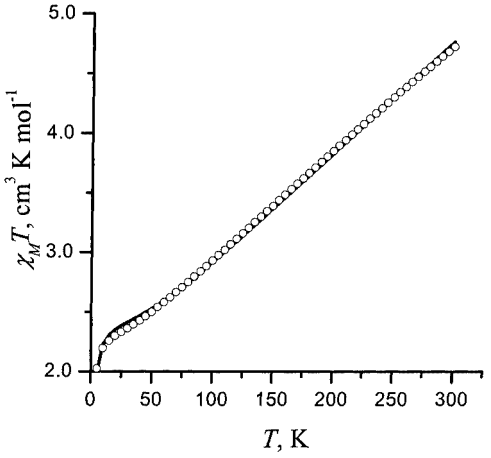

Figure 4. Temperature dependence of the magnetic susceptibility of **2**, plotted as χT vs. T; the solid line is the least-squares fit

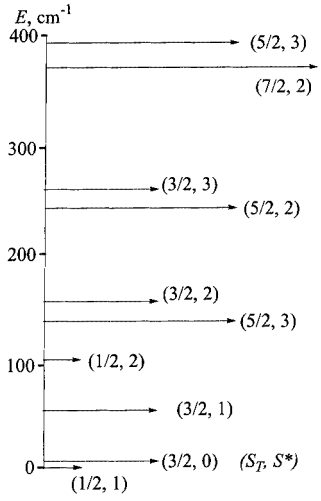

Figure 5. Energy diagram for low-lying spin levels of **2**

cm^3·K·mol^{-1} at 32 K, and after passing through a broad minimum at 50−20 K, increased somewhat again as T approached 5 K Figure 6). Comparison with the calculated spin-only $\chi_M T$ value (9.73 cm^3·K·mol^{-1}) for non-interacting ions again indicates strong antiferromagnetic exchange within the trimetallic species. Two high-spin S = 5/2 iron(III) ions and one high-spin S = 1 nickel(II) ion can couple to give S_T values ranging from 0 to 12/2. Magnetic data were fitted in agreement with the exchange Hamiltonian [Equation (2)] and the expression for $\chi_M T$ [Equation (6)], where $a = -10J_{Fe\text{-}Ni} - 12.5J_{Fe\text{-}Fe}$; $b = 2J_{Fe\text{-}Ni} - 12.5J_{Fe\text{-}Fe}$; $c = 12J_{Fe\text{-}Ni} - 12.5J_{Fe\text{-}Fe}$; $d = {}_{Fe\text{-}Ni} - 2.5J_{Fe\text{-}Fe}$; $e = 2J_{Fe\text{-}Ni} - 2.5J_{Fe\text{-}Fe}$; $f = 10J_{Fe\text{-}Ni} - 2.5J_{Fe\text{-}Fe}$; $\gamma = -6J_{Fe\text{-}Ni} + 5.5J_{Fe\text{-}Fe}$; $h = 2J_{Fe\text{-}Ni} + 5.5J_{Fe\text{-}Fe}$; $\omega = 8J_{Fe\text{-}Ni} + 5.5J_{Fe\text{-}Fe}$; $j = -4J_{Fe\text{-}Ni} + 11.5J_{Fe\text{-}Fe}$; $\kappa = 2J_{Fe\text{-}Ni} + 11.5J_{Fe\text{-}Fe}$; $l = 6J_{Fe\text{-}Ni} + 11.5J_{Fe\text{-}Fe}$; $m = -2J_{Fe\text{-}Ni} + 15J_{Fe\text{-}Fe}$; $n = 2J_{Fe\text{-}Ni} + 15.5J_{Fe\text{-}Fe}$; $o = 4J_{Fe\text{-}Ni} + 15.5J_{Fe\text{-}Fe}$; $p = 17.5J_{Fe\text{-}Fe}$.

$$\chi_M T = (Ng_{mol}^2\beta^2/3k)\cdot(546e^{-a/kT} + 330e^{-b/kT} + 180e^{-c/kT} + 330e^{-d/kT} + 180e^{-e/kT} + 84e^{-f/kT} + 180e^{-\gamma/kT} + 84e^{-h/kT} + 30e^{-\omega/kT} + 84e^{-j/kT} + 30e^{-\kappa/kT} + 6e^{-l/kT} + 30e^{-m/kT} + 6e^{-n/kT} + 6e^{-p/kT})/(13e^{-a/kT} + 11e^{-b/kT} + 9e^{-c/kT} + 7e^{-d/kT} + 11e^{-e/kT} + 9e^{-f/kT} + 7e^{-\gamma/kT} + 5e^{-h/kT} + 9e^{-\omega/kT} + 7e^{-j/kT} + 5e^{-\kappa/kT} + 3e^{-l/kT} + 7e^{-m/kT} + 5e^{-n/kT} + 3e^{-o/kT} + e^{-p/kT}) \quad (6)$$

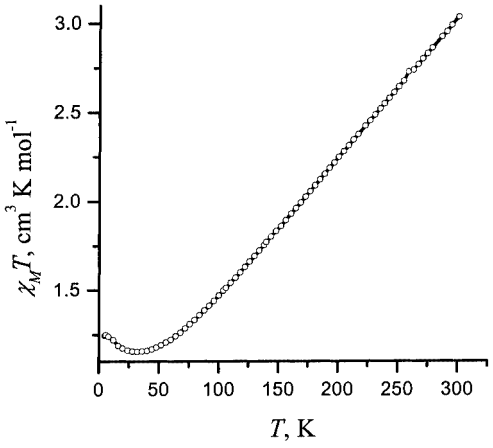

Figure 6. Temperature-dependence of the magnetic susceptibility of **3**, plotted as χT vs. T; the solid line is the least-squares fit

The best fit was obtained with a fixed g_{Fe} value of 2.00 and g_{Ni} = 2.215(2); $J_{Fe\text{-}Fe}$ = −45.60(1) and $J_{Fe\text{-}Ni}$ = −16.96(2) cm^{-1} ($R^2 = 8.54\cdot10^{-5}$). The unexpected shape of the $\chi_M T$ vs. T curve can be clarified from the associated energy diagram for the spin-states (Figure 7). This reveals a (1, 0) ground state, succeeded by the first two excited states (0, 1) and (1, 1), so that there is a diamagnetic state between the two lowest-lying triplet states. When the temperature is decreased, the singlet first excited state becomes populated and the higher states with $S_T \geq 1$ become less populated, reducing $\chi_M T$. However, a further decrease in temperature depopulates this singlet level, in favour of the triplet ground state, so that the reduction in the $\chi_M T$ value with decreasing temperature is thus arrested and reversed.

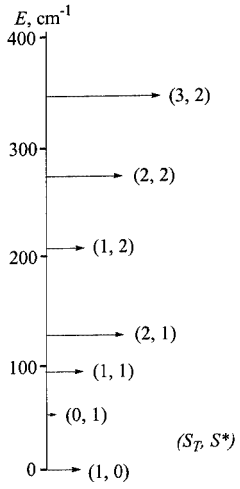

Figure 7. Energy diagram for low-lying spin levels of **3**

When comparing the magnetochemical characteristics of **1**−**3**, one notes that $J_{Fe\text{-}M}$ (M = M^{II}) is insensitive to the identity of M^{II}, whereas the $J_{Fe\text{-}Fe}$ values are affected by the nature of the third metal ion in the triangular skeleton. These results are in agreement with observations by Blake et al.[24] that $J_{Fe\text{-}Fe}$ increases significantly in Fe_2M^{II} relative to that in similar trinuclear (carboxylato)(oxo)iron(III) complexes. It is noteworthy that trinuclear pivalate complexes[28] also show significant antiferromagnetic exchange.

Mößbauer Spectra

The electronic properties of complexes **1**−**3** were examined by ^{57}Fe Mößbauer spectroscopy at 80 and 300 K (Figure 8, Table 5). Each of the spectra display one quadrupole-split doublet. The values of the isomer shifts (IS, δ) and quadrupole splittings (QS) for **1**−**3** are close to those reported previously for similar heterometallic trinuclear complexes,[29] and correspond to a high-spin iron(III) ion. Second-order Doppler effects (an increase in the isomer shift at cryogenic temperature[30]) and Goldanskii−Karyagin anisotropy[30] (manifested by the different relative intensities of the two peaks of the doublet at higher temperatures) are minor, but detectable in the spectra. The data indicate that there is no occurrence of any intermetallic redox process during or subsequent to the synthesis − i.e. there is no electron transfer from M^{2+} (especially from the more readily oxidizable Co^{2+} and Mn^{2+}) to Fe^{3+}. However, the isomer shifts in **1**−**3** are smaller than in some other[31] heterotrinuclear complexes (Table 5), which may be accounted for by the electron-withdrawing nature of the CF_3 group; the decreased donor ability of the carboxylate group thus reduces the electron density in the 3d subshell.[30] Similar effects have been reported for other homopolynuclear iron(III) species.[32,33] The relatively high quadrupole splitting in **1**−**3** also reflects the significant electron-density transfer from the iron(III) centre to the trifluroacetate anion. Previous work[22,31] indicates that quadrupole splitting increases with Fe^{III}−carboxylate bond ionicity.

The Mössbauer results reveal no spin-spin interactions which would be indicative of the exchange coupling that is so compellingly suggested by the magnetic susceptometry.

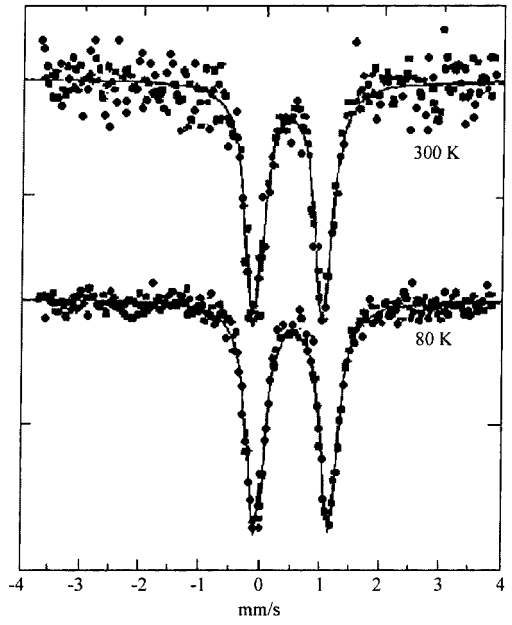

Figure 8. ^{57}Fe Mössbauer spectrum of **1**; the solid line is the least-squares fit; isomer shifts are referred to α-iron at room temperature

The relatively high J values alone lead to the expectation that a "coupled" spectrum might be observed at 80 K. However, similar apparently paradoxical results have been reported by Rentschler and co-workers,[28] who pointed out that they are a consequence of the difference in the experimental time scales of the phenomena on which the two types of measurements are based; the magnetic exchange occurs on a timescale that is too fast to be detected by ^{57}Fe Mößbauer spectroscopy.

Conclusion

Three new heterometallic trinuclear basic trifluoroacetates $[Fe_2M^{II}(\mu_3\text{-}O)(CF_3COO)_6(H_2O)_3]\cdot H_2O$ (M = Mn, Co, Ni) have been prepared. The crystal structures of two complexes were obtained at 100 K. FAB-MS data, IR and UV/

Table 5. Mössbauer spectroscopic parameters of complexes **1**−**3**

Complex	T [K]	IS [Mm/s]	QS [mm/s]	I_1/I_2
$[Fe_2Mn(\mu_3\text{-}O)(CF_3COO)_6(H_2O)_3]\cdot H_2O$	80	0.55	1.38	1.02(6)
	300	0.44	1.22	1.10(6)
$[Fe_2Co(\mu_3\text{-}O)(CF_3COO)_6(H_2O)_3]\cdot H_2O$	80	0.54	1.17	0.89(6)
	300	0.39	0.90	0.91(6)
$[Fe_2Ni(\mu_3\text{-}O)(CF_3COO)_6(H_2O)_3]\cdot H_2O$	80	0.53	1.23	1.01(6)
	300	0.43	1.15	1.05(6)
$[Fe_2^{III}Fe^{II}(\mu_3\text{-}O)(CF_3COO)_6(H_2O)_3]\cdot CF_3COOH$[a]	80	1.51	2.38	Fe^{II}
		0.61	0.97	Fe^{III}
	300	0.75	1.05	−
$[Fe_3(\mu_3\text{-}O)(CH_3COO)_6(H_2O)_3]Cl\cdot 5H_2O$[b]	80	0.71	0.61	−
	30	0.58	0.55	−

[a] K. I. Turte, S. A. Bobkova, R. A. Stukan, *Zh. Neorg. Khimii* **1982**, *27*, 954−960. [b] G. J. Long, W. T. Robinson, W. P. Tappmeyer, D. L. Bridges, *J. Chem. Soc., Dalton. Trans.* **1973**, 573−578.

Vis spectra, along with magnetochemical and Mössbauer studies were interpreted in terms of the trinuclear nature of the compounds. The complexes exhibit substantial intramolecular antiferromagnetic exchange. The absence of any iron(II) centre, as proved by the Mössbauer investigation, showed that no electron transfer from Mn^{II} or Co^{II} to Fe^{III} occurred in these complexes. Increased values of quadrupole splittings are a result of the electron-withdrawing abilities of the CF_3- group in the trifluoroacetate anions.

Experimental Section

General: Reagents and solvents (UkrReaKhim and Merck) were generally used as received. The precursory acetate complexes $[Fe_2^{III}M^{II}(\mu_3\text{-}O)(CH_3COO)_6(H_2O)_3]\cdot 3H_2O$ (M = Mn, Co, Ni) were prepared as described elsewhere.[24]

$[Fe^{III}_2M^{II}(\mu_3\text{-}O)(CF_3COO)_6(H_2O)_3]\cdot H_2O$ (M = Mn, Co, Ni): The initial acetato complex $[Fe_2^{III}M^{II}(\mu_3\text{-}O)(CH_3COO)_6(H_2O)_3]\cdot 3H_2O$ (1.3 g, ca. 2 mmol) was dissolved in aqueous trifluoroacetic acid (15 mL of a 60% solution), and the resulting solution was refluxed for 1 h. After cooling, the reaction mixture was diluted with an equal volume of acetone. Slow concentration of the reaction mixture at room temperature over several days resulted in the formation of red-brown crystals, which were filtered, washed with cold water and dried in vacuo with KOH. Yield: 60−80%.

$[Fe^{III}_2Co(\mu_3\text{-}O)(CF_3COO)_6(H_2O)_3]\cdot H_2O$: $C_{12}H_8CoF_{18}Fe_2O_{17}$ (936.77): calcd. C 15.4, H 0.85, Co 6.30, Fe 11.9; found C 15.3, H 0.83, Co 6.42, Fe 11.6. Yield 1.43 g (75%).

$[Fe^{III}_2Ni(\mu_3\text{-}O)(CF_3COO)_6(H_2O)_3]\cdot H_2O$: $C_{12}H_8F_{18}Fe_2NiO_{17}$ (936.54): calcd. C 15.4, H 0.86, Ni 6.27, Fe 12.0; found C 15.3, H 0.80, Ni 6.40, Fe 11.7. Yield 1.38 g (72%).

$[Fe^{III}_2Mn(\mu_3\text{-}O)(CF_3COO)_6(H_2O)_3]\cdot H_2O$: $C_{12}H_8F_{18}Fe_2MnO_{17}$ (932.76): calcd. C 15.4, H 0.86, Mn 5.89, Fe 12.0; found C 15.4, H 0.88, Mn 5.80, Fe 12.1. Yield 1.26 g (66%).

Physical Measurements: Electronic absorption spectra were recorded with a Carl-Zeiss-Jena Specord-M40 spectrophotometer, IR spectra with a Carl-Zeiss-Jena Specord-75. C,H,N contents were determined using a Carlo Erba 1106 microanalyzer. Mass spectra were obtained with a VG-ZABHF instrument, using 2-nitrobenzyl alcohol as the matrix for the FAB mode. The temperature and field dependencies of the magnetic susceptibilities were measured with an MPMS-5S SQUID magnetometer, Pascal's diamagnetic corrections were applied according to a standard text.[2] Magnetisation experiments were performed at 5 and 300 K. Möβbauer spectra were measured in the transmission mode on conventional spectrometers, a temperature-controlled Leybold cryostat was used for low-temperature spectra. A $3\cdot10^9$ Bq $^{57}Co(Rh)$ sample was used as the γ-ray source, while isomer shifts were referred to α-iron at room temperature. Spectra were deconvoluted using the MossWin program.[34]

X-ray Crystallographic Study: Crystals suitable for crystallography were grown from CH_3NO_2/mesitylene (for the Mn complex) or from $CH_3NO_2/(CH_3)_2CO$/mesitylene layering (for the cobalt complex). A dark red single crystal of **2′** was coated with perfluoropolyether, picked up with a glass fibre and immediately mounted in the cold nitrogen stream to prevent loss of solvent. Intensity data were collected with a Siemens SMART diffractometer at 100 K using graphite-monochromated Mo-K_α radiation (λ= 0.71073 Å). Final cell constants were obtained from a least-squares fit of 4419 reflections. Data collection was performed by hemisphere runs taking frames at 0.3°. A semiempirical absorption correction using the program SADABS[35] was performed on the data set of **2**. Crystallographic data are listed in Table 6. The Siemens SHELXTL1 software package was used for solution, refinement and artwork of the structure. The structure was readily solved by direct methods and difference Fourier techniques. All non-hydrogen atoms except atoms in disordered parts were refined anisotropically and hydrogen atoms were placed at calculated positions and refined as riding atoms with isotropic displacement parameters. Split atom models were used to account for the disorder of the CF_3COO groups and a mesitylene solvent molecule lying on the crystallographic mirror plane. The C−F and F−F distances of the CF_3 groups were re-

Table 6. Crystal data and structure refinement details

	1′	**2′**
Empirical formula	$C_{16}H_{14}N_2O_{21}F_{18}Fe_2Mn$	$C_{25.5}H_{30}O_{19}F_{18}Fe_2Co$
Formula mass	1078.89	1153.13
Crystal system	monoclinic	monoclinic
Space group	*C*2/*c*	*C*2/*m*
a [Å]	22.002(5)[a]	21.426(4)
b [Å]	13.647(3)	15.100(2)
c [Å]	24.767(4)	14.815(3)
β [°]	98.23(3)	117.99(2)
V [Å^3]	7359.9(2)	4232.50(13)
Z	8	4
$\rho_{calcd.}$ [g cm^{-3}]	1.241	1.810
T [K]	100(2)	100
μ [mm^{-1}] (Mo-K_α)	1.16	1.214
Number of reflections collected	11349	8847
Number of independent reflections	6424	3622
Number of parameters	457	346
R_{int}	0.0739	0.0541
R1 (all data)	0.1316	0.0874
wR(F^2) (all data)	0.3665	0.1822

The standard deviations are reported in parentheses.

strained to be equal within errors, and equal displacement parameters were used for the split fluorine atoms. Crystallographic data (excluding structure factors) for the structures reported in this paper have been deposited with the Cambridge Crystallographic Data Centre as supplementary publication no. CCDC-176586. Copies of the data can be obtained free of charge on application to CCDC, 12 Union Road, Cambridge CB21EZ, UK [Fax: 44-1223/336-033; E-mail: deposit@ccdc.cam.ac.uk].

Acknowledgments

V. V. P. acknowledges support from the DAAD foundation and the Max-Planck-Institut für Strahlenchemie. This work was also supported by the Hungarian Science Foundation OTKA No. T034839. A. W. A. thanks Drexel University for support.

[1] *Molecule-based Magnetic Materials* (Eds.: M. M. Turnbull, T. Sugimoto, L. K. Thompson), ACS Symposium Series, USA, **1996**, p. 341.
[2] O. Kahn, *Molecular Magnetism*, VCH Publishers Inc., New York, USA, **1993**, p. 225.
[3] C. M. Davis, A. C. Royer, J. B. Vincent, *Inorg. Chem.* **1997**, *36*, 5316−5320.
[4] M. Fontecave, S. Ménage, C. Doboe-Toia, *Coord. Chem. Rev.* **1998**, *187−188*, 1555−1572.
[5] J. D. Bois, T. J. Mizoguchi, S. J. Lippard, *Coord. Chem. Rev.* **2000**, *200−202*, 443−485.
[6] W.E. Ruettinger, G.C. Dismukes, *Inorg. Chem.* **2000**, *39*, 1021−1027.
[7] D. Gatteschi, R. Sessoli, A. Cornia, *Chem. Commun.* **2000**, 725−732.
[8] V. V. Pavlishchuk, *Teor. Eksp. Khim.* **1997**, *33*, 341−361.
[9] D. Gatteschi, A. Caneschi, R. Sessoli, A. Cornia, *Chem. Soc. Rev.* **1996**, *25*, 101−109.
[10] S. Asirvatham, M. A. Khan, K.M. Nicholas, *Inorg. Chem.* **2000**, *39*, 2006−2007.
[11] H. J. Appley, H.-L. Tsai, N. De Vries, K. Folting, G. Christou, D. N. Hendrickson, *J. Am. Chem. Soc.* **1995**, *117*, 301−317.
[12] R. F. Weinland, E. Gussmann, *Ber. Dtsch. Chem. Ges.* **1909**, *42*, 2997−3005.
[13] R. F. Weinland, H. Holtmeier, *Z. Anorg. Chem.* **1928**, *173*, 49−61.
[14] J. B. Vincent, *Inorg. Chem.* **1994**, *33*, 5604−5606.
[15] S. A. Chavan, D. Srinavas, P. Ratnasamy, *Chem. Commun.* **2001**, 1124−1125.
[16] *Activation and Functionalization of Alkanes* (Ed.: C. L. Hill), John Wiley and Sons, Inc., New York, **1989**, p. 341.
[17] A. R. Schake, H.-L. Tsai, R.J. Webb, K. Folting, G. Christou, D. N. Hendrickson, *Inorg. Chem.* **1994**, *33*, 6020−6022.
[18] S. G. Shova, I. G. Kadelnik, M. Gdanec, Yu. A. Simonov, T. K. Zhovmir, V. M. Meriacre, G. Filotti, K. I. Turte, *Zh. Strukt. Khim.* **1998**, *39*, 917−933.
[19] S. M. Oh, D. N. Hendrickson, K. L. Hassett, R. E. Davis, *J. Am. Chem. Soc.* **1985**, *107*, 8009−8018.
[20] R. D. Shannon, *Acta Crystallogr., Sect. A* **1976**, *32*, 751−755.
[21] T. Sato, F. Ambe, *Acta Crystallogr., Sect. C* **1996**, *52*, 3005−3007.
[22] R. D. Cannon, R. P. White, *Prog. Inorg. Chem.* **1988**, *36*, 195−298.
[23] M. M. Mansurov, O. V. Semenova, S. S. Sokhibov, *Zh. Neorg. Khim. (Russ. Ed.)* **1991**, *36*, 2810−2815.
[24] A. B. Blake, A. Yavari, W. E. Hatfield, C. N. Sethulekshmi, *J. Chem. Soc., Dalton Trans.* **1985**, 2509−2520.
[25] A. B. P. Lever, *Inorganic Electronic Spectroscopy*, 2nd ed., Elsevier, New York, **1984**, p. 334.
[26] C. Fernandes, E. Stadler, V. Drago, C. G. da Cunha, I. N. Kuwabara, *Spectrochim. Acta* **1996**, *A52*, 1815−1821.
[27] C. Kambe, *J. Phys. Soc. Jpn.* **1950**, *5*, 48−55.
[28] E. Rentschler, K. Wieghardt, G. Timko, N. Gerbeleu, *213th National ACS Meeting*, San Francisco, **1997**, INOR 501.
[29] M. K. Johnson, R. D. Cannon, D. B. Powell, *Spectrochim. Acta* **1982**, *38A*, 307−315.
[30] A. Vértes, L. Korecz, K. Burger, *Mössbauer Spectroscopy*, Elsevier, Amsterdam, **1979**.
[31] S. K. Abdulaev, O. A. Nasonova, K. I. Yakubov, K. I. Turte, V. V. Zelentsov, R. A. Stukan, *Zh. Neorg. Khim. (Russ. Ed.)* **1988**, *33*, 1765−1770.
[32] T. Sato, F. Ambe, K. Endo, M. Katada, H. Maeda, T. Nakamoto, H. Sano, *J. Am. Chem. Soc.* **1996**, *118*, 3450−3458.
[33] B. D. Rumbold, G. V. H. Wilson, *J. Phys. Chem. Solids* **1973**, *34*, 1887−1891.
[34] Z. Klencsár, E. Kuzmann, A. Vértes, *J. Radioanal. Nucl. Chem.* **1996**, *A210*, 105.
[35] *SHELXTL*, version 5, Siemens Analytical X-ray Instruments, Inc., Göttingen, **1994**.

Received February 11, 2002
[I02071]